Hindawi
Advances in Materials Science and Engineering
Volume 2018, Article ID 3152170, 7 pages
https://doi.org/10.1155/2018/3152170

Research Article

Formation of Surface Ultrafine Grain Structure and Their Physical and Mechanical Characteristics Using Vibration-Centrifugal Hardening

Volodymyr Kyryliv,[1] **Yaroslav Kyryliv**,[2] **and Nataliya Sas**[3]

[1]*Karpenko Physico-Mechanical Institute of the NAS of Ukraine, 5 Naukova Str., Lviv 79060, Ukraine*
[2]*Lviv State University of Life Safety, 35 Kleparivska Str., Lviv 79007, Ukraine*
[3]*Stepan Gzhytskyi National University of Veterinary Medicine and Biotechnologies, 50 Pekarska Str., Lviv 79010, Ukraine*

Correspondence should be addressed to Volodymyr Kyryliv; kyryliv@ipm.lviv.ua

Received 21 May 2018; Accepted 6 August 2018; Published 23 September 2018

Academic Editor: Laszlo Toth

Copyright © 2018 Volodymyr Kyryliv et al. This is an open access article distributed under the Creative Commons Attribution License, which permits unrestricted use, distribution, and reproduction in any medium, provided the original work is properly cited.

The vibration-centrifugal hardening forms a gradient ultrafine grain structure of the ferritic class with a grain size of 190 nm and a surface microhardness of 8.9 GPa and a depth of up to 6 mm on the surface of 40 Kh steel of the ferritic-pearlitic structure. These parameters are formed due to an increase in the mass of the tool that acts on the processed surface through the balls and depend on the treatment modes. This surface ultrafine grain structure increases the wear resistance properties of steel in oil and oil-abrasive environment and improves the electrochemical characteristics.

1. Introduction

Creation of new materials with predetermined properties is one of the important problems facing modern materials science. Formation of nanocrystalline (NCS) and surface ultrafine grain structures (UFGS) using severe plastic deformation (SPD) is a promising direction for solving this problem. This method obtains volumetric surfaces NCS and UFGS. Obtaining volumetric NCS and UFGS is associated with certain technological difficulties. Therefore, surface treatments for obtaining NCS and UFGS are used more widely. Low-frequency and high-frequency vibration hardening with the balls (VHB) in a special bunker [1–8] are among the known SPD methods of technological improvement of machine components surfaces. However, a depth up to 100 μm of hardened surface layer is insignificant [9], and it does not allow additional finishing operations for high-precision components. It depends on the mass and diameter of the balls, which are interrelated. Small contact loads during treatment, which are difficult to eliminate, should be noted as a shortage of these types of treatment. The developed method of vibration-centrifugal hardening (VCH) deals with an increase of the tool mass without increasing the diameter of the balls, and it can vary within wide limits. Such conditions should lead to an increase in the depth and microhardness of the surface layer by increasing the contact loads in the treatment zone. This causes a hardening of surface layers and an increase of metal structure imperfection and leads to an improvement of its properties. An amplitude and frequency of oscillation, mass of the tool, diameter of the balls, and a treatment time are the main parameters that affect the physical and mechanical properties of the surface layer during vibration treatment.

The purpose of the paper was to investigate a possibility of obtaining surface NCS or UFGS using VCH and to explore their physical, mechanical, and electrochemical properties.

2. Materials and Methods

40 Kh (0.4C–1Cr) steel was chosen as the material for the study—the rings with outer and inner diameters of 75 and

60 mm, respectively, and 20 mm in width were made of this steel. The inserts were made of 40 Kh steel in the state of delivery. Hardened rings were made of the same steel for comparative studies of wear resistance, which reach the hardness of HRC 52–54, and were heat-treated and strengthened after VCH rings were abraded to a surface roughness Ra = 0.8–1.2 μm. Strengthening was carried out on a special vibration-centrifugal hardening research unit (Figure 1) with a special massive tool using balls with a diameter of 13 mm fixed in it. The unit provides vibrations of a certain amplitude and rotation of the tool, as well as its movement along the cylindrical surface being processed. Samples were fixed on a mandrel. The treatment was performed with the following parameters: amplitude of oscillation $A = 5$ mm; frequency of oscillations $f = 24$ Hz; working tool mass $m = 3.5$–7.5 kg; treatment time $\tau = 12$–36 min; and eccentricity $\varepsilon = 10$ mm.

During the VCH treatment, shock dynamic loads act on the surface of a cylindrical sample that carries out vibration oscillations of a certain amplitude and frequency. The loads are made by a special tool of increased mass in the form of a ring with balls fixed in it, which rolls along the outer cylindrical surface of the sample.

During the process, sample 1 is fixed by the brackets 2 located on the common platform 3. The tool 4 with the balls 5, which have rotational orientation around of their own geometric axis, is freely placed on the outer surface of the sample. They are evenly placed along the rim of the ring. Balls' hardness (HRC 60–62) is higher than the material sample hardness. Under the influence of vibration, the tool 4 rotates and moves along the generatrix of the sample surface. Speed of rotation around the axis of the sample depends on the frequency and amplitude of the oscillations. At each time point, one of the balls of the tool contacts with the surface of the sample. Every contact with the ball occurs with impact, and the bodies that collide are a massive tool and the treatment sample. The impact interaction between the tool and the sample forms large contact stresses in the surface layer of the sample material at the contact points. The sample material is strengthened as a result of SPD. The instrument design and its mass make it possible to obtain high contact loads at constant size of balls and also provide a fixed direction of movement of the balls with a mandrel in the radial direction to the sample, which increases the depth of the hardening.

X-ray studies of the obtained structure were carried out on an X-ray diffractometer DRON-3 in CuKα radiation ($U = 30$ kV, $I = 20$ mA) with the steps of 0.05° and the exposure at point 4 s. The diffractograms were processed using the CSD software package [10]. X-ray patterns were identified by JCPDS-ASTM card files [11]. The grain size was calculated by the size of the coherent scattering regions and using Selyakov–Scherrer formula. Microhardness was measured with a PMT-3 unit at a load of 100 g. The microstructure was investigated on EVO 40XVP scanning electron microscope. The study of wear resistance properties and the determination of the friction coefficient were carried out on a MI-1M friction machine using a ring-insert scheme in an oil and oil-abrasive environment. The sample rings were 75 mm in diameter [12]. Slavol M-3042 TU 13932946.015-96 with addition of 0.1 weight percent of quartz sand (up to 40 μm) was used as oil at 2.0 MPa load and a sliding speed of 0.9 m/s. Weight loss for an appropriate period of time (2 hours) was assumed as the criterion of wear. Weighing of the samples was carried out on analytical scales VLA-20g-M with accuracy of ±4 mg.

Electrochemical investigations were carried out on potentiostats P-5827M and P-5848 using a three-electrode scheme: a sample-working electrode, an auxiliary platinum electrode, and a reference silver chloride-saturated electrode [13].

3. Results and Discussion

The results in [13] show that the optimum parameters allowing to obtain high microhardness and hardening depth are as follows: amplitude of oscillation $A = 5$ mm; frequency of oscillations $f = 24$ Hz; working tool mass $m = 4.5$ kg; treatment time $\tau = 28$ min; and eccentricity $\varepsilon = 10$ mm. Due to such design of the tool and the use of optimal parameters, the VCH provides the formation of a ferritic class UFGS (Figures 2 and 3) with a grain size on the surface up to 190 nm, a high density of dislocations, and microstresses in the lattice (Figure 4).

Figure 2 shows the structure of steel after the VCH treatment at depths of 100 and 500 μm and the initial lattice structure. The steel structure is formed under optimal time conditions (Figure 5, curve 4).

After the VCH, the microstructure is highly fragmented near the surface at a depth of 100 μm (Figure 2(a)). The grains are fragmented unevenly by separate blocks. At a depth of 500 μm (Figure 2(b)), the picture is similar, and the distribution of grain size decreases apparently due to a more even distribution of deformation during the impact of the balls' surfaces.

Results of X-ray diffraction studies of the optimal mode of the VCH (28 min) showed that the structure dispersion on the surface reaches 190 nm, and the dislocation density is 0.84×10^{12} cm^{-2}. One α-phase can be seen in the initial ferritic-pearlitic structure. There are no cementite lines on X-ray patterns (Figure 3), which agrees well with [14, 15] on the decomposition of cementite as a result of cold plastic deformation.

In conditions typical for a VCH, such decomposition is possible also at temperatures below the austenite phase existence. The ferrite structure was detected by X-ray studies at all depths within the range of 1 mm. The nature of the lines (110) and (220) indicates large stress in the lattice of the deformed metal (Figures 3 and 4). The density of dislocations in the 1 mm section decreases gradually the depth of the metal and this provides a gradient character of the grain size increase. The main increase in microhardness was obtained due to large stresses (0.106%) in the lattice (Figure 4). The UFGS has an increased lattice parameter, which decreases depth (Figure 4). Carbon may segregate at grain boundaries and on dislocation cores or in the form of small graphite precipitates and small residual parts of cementite. Dissolution of cementite during the cold deformation leads

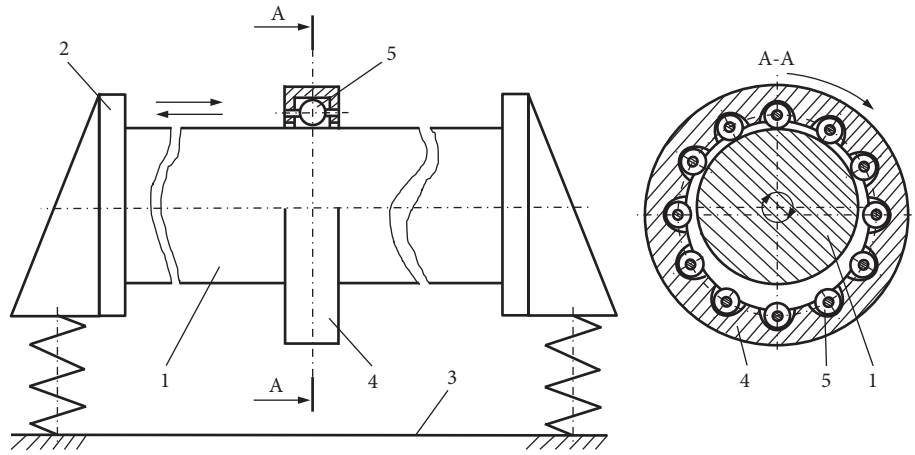

Figure 1: Scheme of VCH of external cylindrical surfaces: (1) sample; (2) brackets; (3) the common platform; (4) tool; (5) balls.

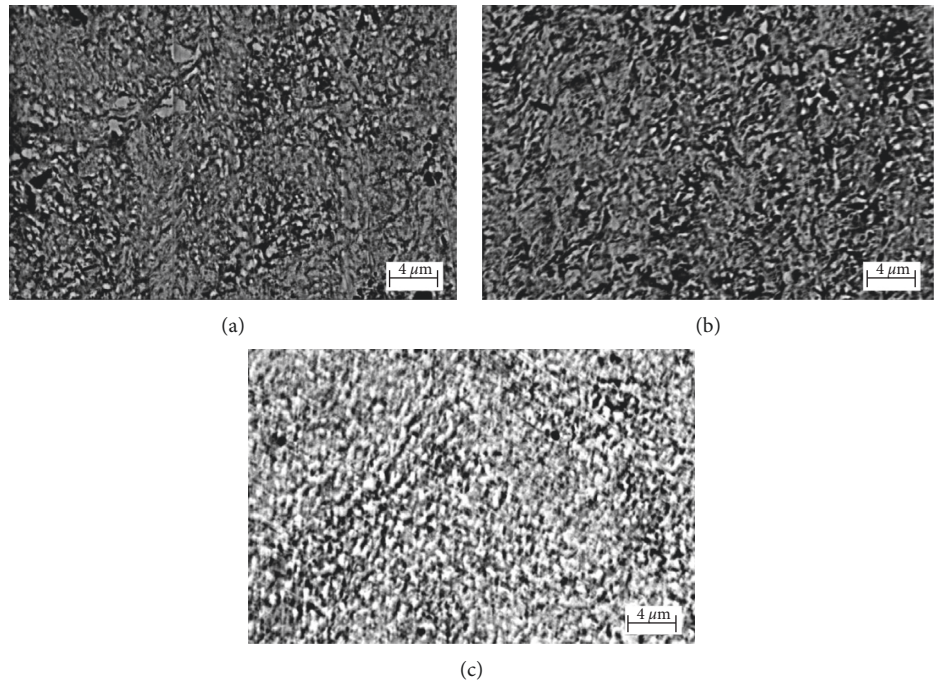

(a) (b)

(c)

Figure 2: The structure of 40 Kh steel at the optimum parameters after VCH at depths of (a) 100 and (b) 500 μm and (c) the initial lattice structure.

to redistribution of carbon, which, being placed on the grain boundaries, plays the role of "useful impurities" and blocks the returning processes. As a result of cold SPD at VCH, the initial ferrite-pearlite structure is transformed into a ferrite structure.

The influence of the treatment time on microhardness and depth of strengthening of 40 Kh steel was investigated in [13]. The duration of treatment varied from 6 to 36 min. This treatment time was selected experimentally. It was showed that after 6 min of treatment, the microhardness of the surface layer is relatively low (5.8 GPa), and after more than 36 min, a repeening occurs in the surface layer and the surface collapses. Microhardness of a hardened surface layer essentially depends on the treatment time (Figure 5) and reaches up to 8.9 GPa, and its depth reaches up to 6 mm at these modes. The treatment time of 28 min is optimal for 40 Kh steel. However, low-frequency VHB makes it possible to reach 11.5 GPa at a much smaller depth, not exceeding 100 μm [5]. This is evidently caused by the multidirectional deformation due to the chaotic distribution of the balls' impacts direction in a special bin during a low-frequency VHB in comparison with the VCH.

The surface UFGS of the sample obtained under optimal conditions was investigated for wear resistance and corrosion-electrochemical characteristics. Uniform hardened layer on the surface of the sample increases the wear

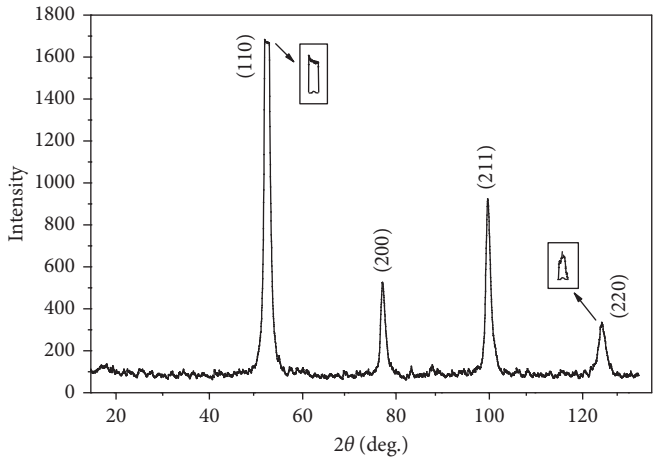

Figure 3: The diffractogram of 40 Kh steel after the VCH at a depth of 100 μm.

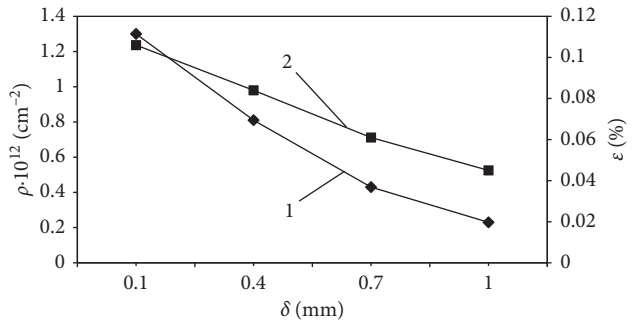

Figure 4: Changes of dislocation density (1) and relative deformation of the lattice (2) along a depth δ of the strengthened layer.

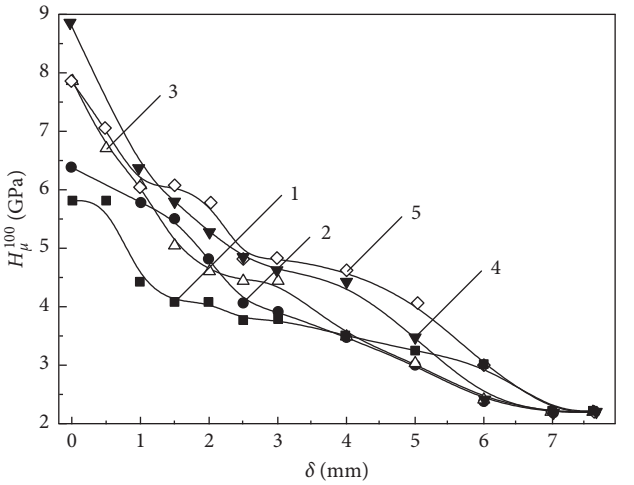

Figure 5: Microhardness of 40 Kh steel after the VCH with duration of treatment: (1) 6; (2) 12; (3) 20; (4) 28; (5) 36 min.

resistance under conditions of oil wear (Figure 6) and oil-abrasive wear (Figure 7), respectively, in 1.6 and 1.4 times. It also increases the wear resistance of unstable inserts by reducing the friction coefficient of the pair from 0.18 (for hardened samples) to 0.07 (for samples with surface UFGS) (Figure 8). The main factors that cause an increase of wear resistance are increased microhardness and low coefficient of friction of the surface with UFGS [12, 16, 17]. The results obtained for increasing wear resisting properties of the inserts are in good agreement with [12, 16, 17], where the increase in wear resistance of both rings and inserts is shown in the case of hardening treatment made only for rings.

Resistance to corrosion damage is also a very important characteristic of the material. Investigation of the polarization curves of hardened samples compared with the annealed ones showed that the change in the technological parameters of the VCH treatment (weight of the working tool, treatment time, etc.) affects differently both the degree of deformation of steel 40 Kh and its corrosion-electrochemical behavior. VCH with 3.5 kg working tool showed no significant difference in the nature of the polarization curves depending on the treatment time [13].

Using 4.5 kg working tool (Figure 9) allowed obtaining the differences in the corrosion-electrochemical characteristics depending on the treatment time. A comparison of the polarization curves for different durations of the VCH (6–20 min) for a given tool mass (Figure 9) showed a noticeable change in the character of the polarization curves, in particular their anode branches. With treatment time of 20 min, the anode current densities decrease by almost an order of magnitude, and the polarization resistance is 72.79 MΩ/m^2 (Table 1), which exceeds the normalized state (64.23 MΩ/m^2), while corrosion potential E_{cor} almost does not differ from the normalized state. Such behavior can be explained by the fact that the VCH generates residual compressive stresses over the entire depth of the hardened layer, whereas after mechanical treatment tensile stresses of considerable magnitude are formed [18]. The positive effect of the strengthened VCH layer can be associated with an increase in the number of adsorption centers. The improvement in corrosion characteristics can also be attributed to the diffusion of chromium along the grain boundaries into the UFGS, leading to the formation of a chromium-rich passivation layer. Increase in treatment time up to 28 min (at $m_i = 4.5$ kg) provides the maximum value of microhardness at the optimum depth of the hardened layer (Figure 9), but the electrochemical characteristics under this mode deteriorate significantly: R_p decreases to 31.69 MΩ/m^2 (Table 1), E_{cor} shifts to the negative side (−0.490 V), and the polarization curves do not differ from the state after mechanical treatment (Figure 9).

Thus, the conducted studies show that the VCH provides forming a gradient UFGS of a considerable depth and high microhardness on the steel surface. These parameters, along with the corrosion and electrochemical characteristics, depend on the modes of the VCH. Such UFGS provides better wear resistance properties. The large depth of hardening is an essential advantage of the developed method of VCH, which makes it possible to carry out finishing operations for precision machine parts.

4. Conclusions

(1) The results, presented in the article, prove that VCH makes it possible to obtain a gradient UFGS with

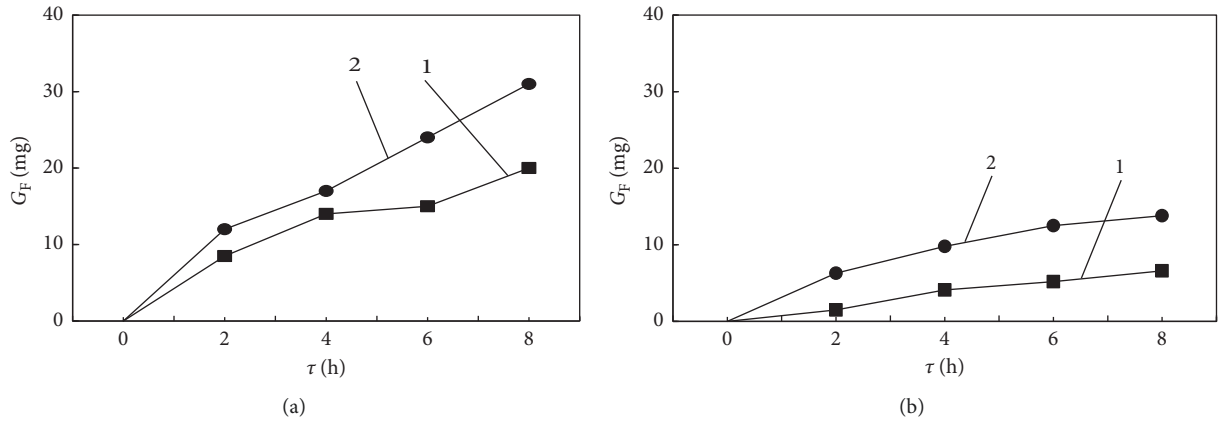

Figure 6: Wearing kinetics for friction pair 40 Kh steel-40 Kh steel after VCH and hardening ((a) ring; (b) insert) under a load of 2 MPa in the oil environment: (1) VCH; (2) hardening with low tempering (200°C).

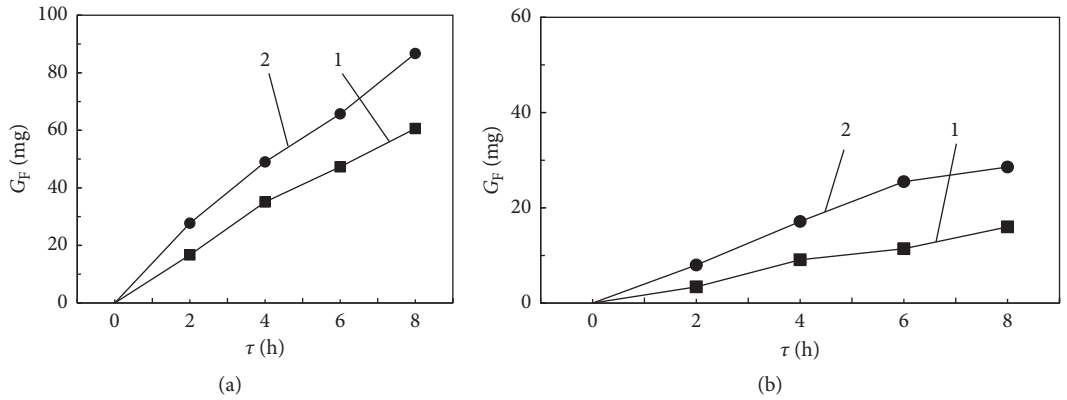

Figure 7: Wearing kinetics for friction pairs made of 40 Kh steel-40 Kh steel after the VCH and hardening ((a) ring; (b) insert) under a load of 2 MPa in an oil-abrasive environment: (1) VCH; (2) hardening with low tempering (200°C).

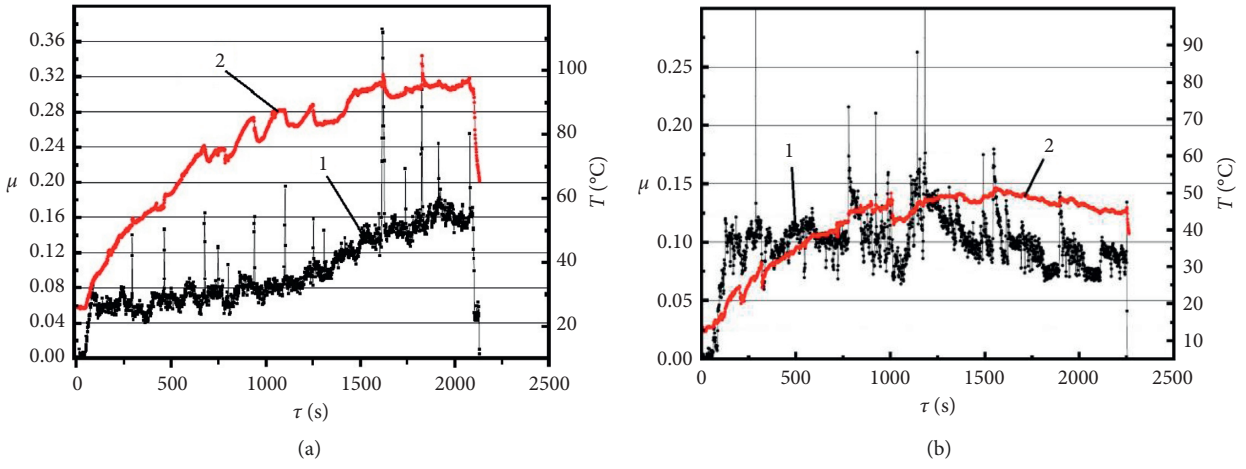

Figure 8: Friction coefficient (1) and temperature (2) for pairs made of steels 40 Kh-40 Kh after hardening ring (a) and the processed VCH (b).

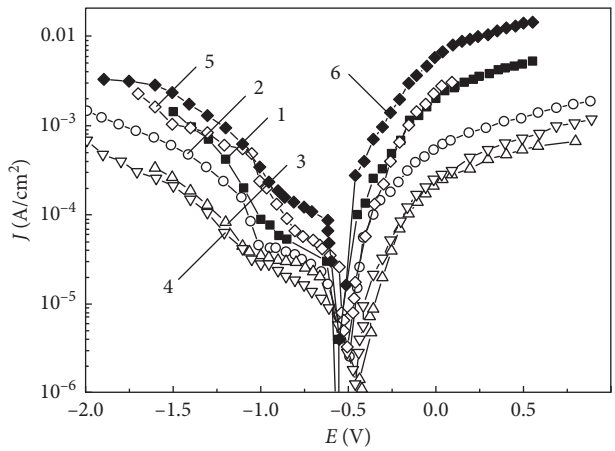

Figure 9: Polarization curves of 40 Kh steel after normalization and the VCH (a working tool weight of 4.5 kg) for different treatment times: (1) after normalization; (2) 6; (3) 12; (4) 20; (5) 28; (6) 36 min.

Table 1: Mechanical and electrochemical characteristics of 40 Kh steel after VCH.

Number	Sample state		Surface microhardness H_μ^{100} (GPa)	Maximum hardening depth δ (mm)	$-E_{cor}$ (V)	R_p (MΩ/m^2)	I_a^{max} (A/cm^2)
	Treatment	Treatment time τ (min)					
1	Normalization	—	2.25	—	0.43	64.23	0.0020
2	VCH (tool mass 4.5 (kg))	6	5.83	5.4	0.47	25.66	0.00057
3		12	6.43	5.4	0.39	68.06	0.00024
4		20	7.94	6.4	0.44	72.79	0.00027
5		28	8.91	5.8	0.49	31.69	0.0030
6		36	7.94	6.4	0.57	16.83	0.0064

high microhardness (up to 8.9 GPa) and hardening depth (up to 6 mm) due to increasing the tool mass. It allows carrying out finishing operations for precision machine parts. Under optimal conditions, VCH generates on the 40 Kh steel ferritic UFGS with a grain size up to 190 nm from the original ferritic-pearlitic structure.

(2) The parameters of the strengthened layer depend on the modes of the VCH, in particular on the weight of the tool and the treatment time. It is shown that, under optimal treatment conditions, wear resistance of samples with surface UFGS increase in 1.6 times (oil environment) and in 1.4 times (oil-abrasive environment) in comparison with hardened samples. At the same time, the wear resistance of the unstressed inserts increases due to the reduction of the friction coefficient of the pair.

(3) For optimal modes of vibration-centrifugal hardening, the corrosion and electrochemical characteristics of the surface layer are improved.

Data Availability

The data used to support the findings of this study are available from the corresponding author upon request.

Conflicts of Interest

The authors declare that there are no conflicts of interest regarding the publication of this paper.

Authors' Contributions

VK investigated the microhardness, friction coefficient, and corrosion-electrochemical characteristics. He directed the study and analyzed the obtained results from the point of practical application. YK developed the plan of the study, carried out the general analysis of the results, and prepared the article. He also chose regimens and carried out the strengthened treatment. NS explored the ultrastructure by using physical methods of investigations and carried out the wear resistance tests. All authors read and approved the final manuscript.

References

[1] L. H. Zhu, Y. J. Guan, Y. J. Wang, Z. D. Xie, and J. Lin, "Influence of process parameters of ultrasonic shot peening on surface nanocrystallization and hardness of pure titanium," *International Journal of Advanced Manufacturing Technology*, vol. 89, no. 5–8, pp. 1451–1468, 2017.

[2] A. Karimi and S. Amini, "Steel 7225 surface ultrafine structure and improvement of its mechanical properties using surface

nanocrystallization technology by ultrasonic impact," *International Journal of Advanced Manufacturing Technology*, vol. 83, no. 5–8, pp. 1127–1134, 2016.

[3] X. Zhao, B. Zhao, Y. Liu, Y. Cai, and C. Hu, "Research on friction and wear behavior of gradient nanostructured 40Cr steel induced by high frequency impacting and rolling," *Engineering Failure Analysis*, vol. 83, pp. 167–177, 2018.

[4] X. Mao, H. Liang, Z. Wang, and L. Shao, "Enhancement of mechanical properties and corrosion resistance of low-carbon steel with gradient microstructure by impact peening and recovery treatment," *Surface Review and Letters*, vol. 25, no. 2, article 1850048, 2018.

[5] N. R. Tao, J. Lu, and K. Lu, "Surface nanocrystallization by surface mechanical attrition treatment," *Materials Science Forum*, vol. 579, pp. 91–108, 2008.

[6] Y. He, K. Li, I. S. Cho et al., "Microstructural characterization of SS304 upon various shot peening treatments," *Applied Microscopy*, vol. 45, no. 3, pp. 155–169, 2015.

[7] Y. Todaka, M. Umemoto, J. Yin, Z. Liu, and K. Tsuchiya, "Role of strain gradient on grain refinement by severe plastic deformation," *Materials Science and Engineering A*, vol. 462, no. 1-2, pp. 264–268, 2007.

[8] R. Peng, L. C. Fu, and L. P. Zhou, "Improved wear resistance by phase transformation of surface nanocrystalline 1090 steel prepared by sandblasting technique," *Applied Surface Science*, vol. 388, pp. 406–411, 2016.

[9] W. Lei, Y. Yong, W. Yaming, and J. Ying, "Effect of nanocrystalline surface and iron-containing layer obtained by SMAT on tribological properties of 2024 Al alloy," *Rare Metal Materials and Engineering*, vol. 44, no. 6, pp. 1320–1325, 2015.

[10] W. Krous and G. Nolze, "Powder cell–a program for the representation and manipulation of crystal structures and calculation of the resulting X-ray powder patterns," *Journal of Applied Crystallography*, vol. 29, no. 3, pp. 301–303, 1996.

[11] L. G. Akselrud, P. Y. Zavalii, Y. N. Gryn, V. K. Pecharski, B. Baumgartner, and E. Wölfel, "Use of the CSD program package for structure determination from powder data," *Materials Science Forum*, vol. 133–136, pp. 335–342, 1993.

[12] H. Nykyforchyn, V. Kyryliv, and O. Maksymiv, "Wear resistance of steels with surface nanocrystalline structure generated by mechanical-pulse treatment," *Nanoscale Research Letters*, vol. 12, no. 1, pp. 150–154, 2017.

[13] I. S. Aftanaziv, A. I. Bassarab, and Y. B. Kyryliv, "Mechanical and corrosion characteristics of 40Kh steel after vibration-centrifugal hardening treatment," *Materials Science*, vol. 38, no. 3, pp. 436–441, 2002.

[14] R. Hossain, F. Pahlevani, E. Witteveen et al., "Hybrid structure of white layer in high carbon steel–formation mechanism and its properties," *Scientific Reports*, vol. 7, no. 1, article 13288, 2017.

[15] Y. J. Li, P. Choi, C. Borchers et al., "Atomic-scale mechanisms of deformation-induced cementite decomposition in pearlite," *Acta Materialia*, vol. 59, no. 10, pp. 3965–3977, 2011.

[16] V. I. Kyryliv, "Improvement of the wear resistance of medium-carbon steel by nanodispersion of surface layers," *Materials Science*, vol. 48, no. 1, pp. 119–123, 2012.

[17] V. I. Kyryliv, B. P. Chaikovs'kyi, O. V. Maksymiv, A. V. Shal'ko, and P. Y. Sydor, "Serviceability of 60KH2M roll steel with surface nanostructure," *Materials Science*, vol. 52, no. 6, pp. 848–853, 2017.

[18] B. Chen, B. Huang, H. Liu, X. Li, M. Ni, and C. Lu, "Surface nanocrystallization induced by shot peening and its effect on corrosion resistance of 6061 aluminum alloy," *Journal of Materials Research*, vol. 29, no. 24, pp. 3002–3010, 2014.